VOL. 18, NO. 11, JUNE 2023 ISSN 1819-6608
ARPN Journal of Engineering and Applied Sciences

www.arpnjournals.com

THE EFFECT OF TEMPERATURE ON THE HYDROTHERMAL SYNTHESIS OF CARBONATED APATITE FROM CALCIUM CARBONATE OBTAINED FROM GREEN MUSSELS SHELLS

Deni Fajar Fitriyana[1], Agustinus Purna Irawan[2], Aldias Bahatmaka[1], Rifky Ismail[3,4], Athanasius Priharyoto Bayuseno[3], Rilo Chandra Muhamadin[4,5], Tezara Cionita[6], Januar Parlaungan Siregar[7], Emilianus Jehadus[8], Gregorius Dimas Baskara[9], Dwinta Laksmidewi[10], and Natalino Fonseca Da Silva Guterres[11]

[1]Department of Mechanical Engineering, Faculty of Engineering, Universitas Negeri Semarang, Semarang, Indonesia
[2]Faculty of Engineering, Universitas Tarumanagara, Jakarta Barat, Indonesia
[3]Department of Mechanical Engineering, Faculty of Engineering, Diponegoro University, Semarang, Indonesia
[4]Center for Biomechanics, Biomaterial, Biomechatronics, and Biosignal Processing (CBIOM3S), Diponegoro University, Semarang, Indonesia
[5]Department of Mechanical Engineering, Faculty of Engineering, Universitas Muhammadiyah Gresik, Gresik, Indonesia
[6]Faculty of Engineering and Quantity Surveying, INTI International University, Nilai, Negeri Sembilan, Malaysia
[7]Faculty of Mechanical & Automotive Engineering Technology, Universiti Malaysia Pahang, Pekan, Pahang, Malaysia
[8]Mathematics Education Department, Universitas Katolik Indonesia Santu Paulus Ruteng, Indonesia
[9]School of Electrical Engineering and Informatics, Institut Teknologi Bandung, Bandung, Indonesia
[10]Faculty of Economics and Business, Universitas Katolik Indonesia Atma Jaya, Jl. Jenderal Sudirman, Jakarta, Indonesia
[11]Department of Mechanical Engineering, Dili Institute of Technology, Ai-meti Laran Street, Dili, Timor-Leste
E-Mail: deniifa89@mail.unnes.ac.id

ABSTRACT

Hydroxyapatite (HAp) refers to a bioceramic broadly employed in bone tissue engineering since it has bioactive and osteoconductive properties. The synthesis of HAp will be more economically viable using waste materials because it is cheap, easy to find, and available in large quantities. Therefore, this study aimed to synthesize and characterize HAp from green mussel shells by hydrothermal method at various temperatures. Precipitated calcium carbonate (PCC), made from green mussel shell powder, is employed in this study. Utilizing a hydrothermal reactor for 14 hours at 120℃, 140℃, as well as 160℃, a combination of PCC and $(NH_4)_2HPO_4$ with a Ca/P molar ratio of 1.67 was synthesized to form HAp. Note that the synthesis findings were categorized using scanning electron microscopy (SEM), Fourier transforms infrared spectroscopy (FTIR), as well as X-ray diffraction (XRD) tests. Apart from that, the FTIR test showed the formation of HAp in all test variations because the results of –OH, and $–PO_4$ were found. XRD results that have been analyzed using HighScore Plus software show the percentage of weight (%) and crystal size of HAp increases with increasing hydrothermal temperature. Other than that, HAp produced at hydrothermal temperature variations of 160℃ has a hexagonal crystal system with a percentage of weight (%) as well as a crystal size of 46.43 nm and 99.3%, whilst the amount of impurity (%) produced is 0.7%. The higher the hydrothermal temperature, the weight percentage (%), and the crystallite size in HAp are getting bigger while the number of impurities gets smaller.

Keywords: precipitated calcium carbonate (PCC), green mussel shells, hydrothermal, hydroxyapatite.

Manuscript Received 22 February 2023; Revised 26 July 2023; Published 13 August 2023

INTRODUCTION

Food waste, such as egg shells, bones, and seafood shells, is generally disposed of in landfills. Improper management of food waste will have several negative environmental consequences, such as the emergence of pathogens, the emission of strong odors, and environmental pollution. Motivated by environmental and economic concerns, a significant amount of research effort has been directed into the proper management and recycling of these by-products to reduce waste output. In many circumstances, these by-products can be used as a potential precursor to being turned into value-added goods, such as calcium phosphate materials [1], [2]. Hydroxyapatite (HAp) is a member of the calcium phosphate family [1]. Hydroxyapatite (HAp) refers to one of the biomaterials employed as biomedical materials, for instance, drug delivery systems, bone tissue repair, bioactive implant coatings, as well as bone fillers [3]. It happens because HAp is known to have good biocompatibility, bioactivity, and osteoconductivity. Furthermore, HAp can accelerate the healing of damaged bone tissue because it is easily accepted in bone tissue (immunogenic), is non-toxic, non-inflammatory, and has a chemical content similar to human bone [4].

Green mussel is a marine species that the majority of Indonesians consume. In many Indonesian coastal regions, the cultivation of green mussels is prevalent. The significant public interest in consuming mussels makes them a marketable commodity [5]. However, in Indonesia, it is still uncommon to utilize

green mussel shell waste. In contrast, green mussel shell waste has enormous potential as a basic material for HAp synthesis because of its high level of $CaCO_3$ content [6], [7]. According to research conducted by Borciani *et al*., the major component of marine shell trash, including green mussel shells, is $CaCO_3$ (95-98%). In general, between 59% and 75% of green mussel shells are discarded, while the remaining portion is edible [8]. There have been recent studies on the advantages of using marine biological waste as a calcium source for the synthesis of hydroxyapatite (HAp). Some of the key advantages include:

a) Improved biocompatibility: HAp synthesized from marine biological waste has been shown to have improved biocompatibility compared to HAp synthesized from other sources, making it a promising material for biomedical applications [1], [2], [9], [10].
b) Better control of particle size and morphology: Marine biological waste has a naturally occurring microstructure that can be preserved during the HAp synthesis process, resulting in HAp particles with controlled size and morphology. This is advantageous for applications such as drug delivery and tissue engineering [2].
c) Higher purity and better crystallinity: Marine biological waste have been found to have higher calcium carbonate ($CaCO_3$) content, resulting in higher purity and better crystallinity of the synthesized HAp [6]–[8], [11].
d) More sustainable and environmentally friendly: The use of marine biological waste as a calcium source is more sustainable and environmentally friendly compared to the mining and processing of limestone or other geological minerals. Contribute to reducing environmental impact by converting waste into value-added biomaterials and moving global society towards zero waste [12]–[14].
e) Low cost: The use of marine biological waste as a calcium source is relatively inexpensive compared to other sources. Clamshells are a readily available and abundant resource and do not require significant processing or transportation costs. Additionally, the use of marine biological waste as a precursor is a sustainable and environmentally friendly approach to HAp synthesis, as they are a waste product of the seafood industry and can be obtained at low cost [1], [13]–[15].

Hydrothermal synthesis is a method of single-crystal synthesis that relies on the solubility of minerals in hot water under high pressure. Crystal growth during the synthesis process occurs in a steel pressure vessel called an autoclave, where nutrients are supplied along with water [16], [17]. Since it can form HAp with high crystallinity, the hydrothermal approach is frequently utilized in the HAp production process. Parameters in the hydrothermal process, such as pH, holding time, and temperature, greatly determine crystallinity, crystal size, morphology, and the amount of impurities in the resulting HAp [18]-[21]. Research on the hydrothermal temperature effect concerning the HAp characterization produced has been extensively studied in previous studies. Onoda *et al*. (2016) compared the synthetic characteristics of HAp made from corbicula shells and commercial calcium carbonate ($CaCO_3$) employing the hydrothermal technique. In this investigation, hydrothermal was conducted for 1, 3, and 6 hours at varying temperatures of 120°C, 140°C, 160°C, as well as 180°C. The HAp peak produced by commercial $CaCO_3$ samples had a higher intensity, according to the findings of the X-ray diffraction (XRD) test than the HAp peak of the corbicula shells samples [22].

Therefore, high purity and crystallinity HAp may be created by synthesizing it with precipitated calcium carbonate (PCC) from recycled seashells [6], [23]. Aziz et al. also utilize hydrothermal techniques for the synthesis of HAp from PCC extracted from Anadara granosa shells. The hydrothermal reaction was conducted in an autoclave for 16 to 32 hours at 140°C, 160°C as well as 180°C. Note that the best HAp was achieved at 140°C temperature with a 16-hour holding time. XRD test findings indicated the nano-sized pure HAp formation has high crystallinity and uniform size distribution [23]. The HAp synthesis employing 1.73 g H_3PO_4 as well as 5.905 g $Ca(NO_3)_2$ $4H_2O$ by hydrothermal method with a temperature of 140-220°C for 1-12 hours has been studied by Zhu et al. The hydrothermal process performed for 8 hours at 200°C produced the best quality HAp [24].

The potential for HAp applications in Indonesia is tremendously wide, considering the increasing amount of people with bone diseases [21]. However, the limited number of domestic HAp producers causes high imports. Other than that, the total imports of HAp in 2018, 2019, and 2020 were 980.73 tons, 734.92 tons, and 631.76 tons, with a total import value of 5,708.035 (US$) [25]. The use of precipitated calcium carbonate (PCC) from green mussel shells with a predominance of vaterite crystal phase as a raw material for the synthesis of HA by the hydrothermal method has not been studied extensively. Vaterite is the most unstable polymorph of calcium carbonate with a hexagonal crystal structure that can be used as a precursor for the synthesis of hydroxyapatite. Vaterite is utilized in biomaterial applications including abrasives, bone substitutes, and drug delivery systems. To enhance the creation of carbonate apatite, porous structures, and pure vaterite are favored in the development of bone substitutes [26]. According to a study conducted by Tanaka *et al*., the remodeling of carbonate apatite into new bone was accelerated when vaterite was utilized as a precursor as compared to calcite. Based on their findings, vaterite may be a more suitable precursor than calcite for the production of carbonate apatite artificial bone [27]. Therefore, this study will investigate the process of synthesizing HAp using PCC with a predominance of vaterite crystal phase as the base material from green mussel shells at a variety of

hydrothermal temperatures (140°C, 160°C, as well as 180°C) for 14 hours.

MATERIALS AND METHODS

The precipitated calcium carbonate (PCC) from green mussel shells in this study was obtained from the Center for Bio Mechanics, Bio Material, Mechatronics, and Bio Signal Processing (CBIOM3S), the Diponegoro University, Semarang, Indonesia. The chemical composition of the PCC is shown in Table-1 [28], [29].

Table-1. PCC chemical composition of green mussel shells.

Element	Composition (wt.%)
C	14.11
O	52.41
Ca	33.48
Total	100

Figure-1 depicts the results of the Rietveld analysis performed on the XRD diffractogram of the PCC utilized in this investigation using the Highscore Plus version 3.0e software. The crystal phase contained in PCC from green mussel shells is vaterite, aragonite, as well as calcite. Vaterite has a weight percentage (%), a crystallite size of 91.2%, and 34 nm with a monoclinic crystal system. Meanwhile, aragonite and calcite had weight percentages (%) of 3.9% and 4.9%, respectively.

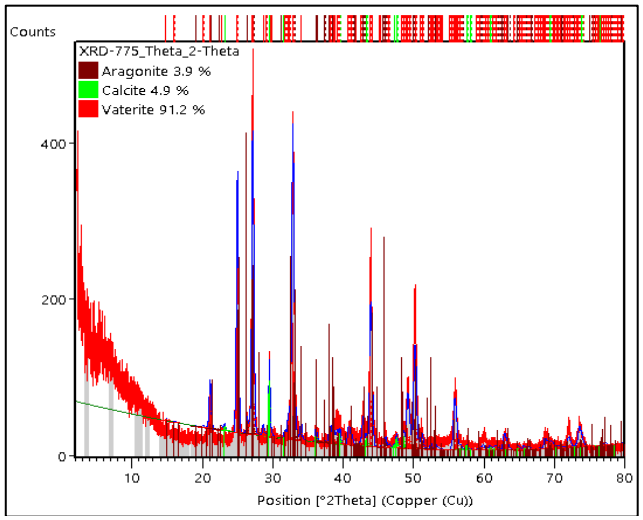

Figure-1. XRD Patterns of PCC from green mussel shells.

The analytical reagent (AR) grade diammonium hydrogen phosphate ($(NH_4)_2HPO_4$) and ammonium hydroxide (NH_4OH) produced by Merck were used as initial precursors for obtaining hydroxyapatite (HAp) in this study. The experimental setup is shown in Figure-2. The synthesis of HAp was conducted by mixing $(NH_4)_2HPO_4$ and PCC at a 1.67 Ca/P molar ratio (5 g of PCC and 3.96 g of $(NH_4)_2HPO_4$) and then added NH4OH 25% (Merck) to produce a mixed pH of 12. The solution was stirred utilizing a magnetic stirrer for 30 minutes at rpm and temperature of 300 rpm and 30°C. Consequently, the synthesis process using the hydrothermal method was carried out for 14 hours of 120°C, 140°C, as well as 160°C temperature variations.

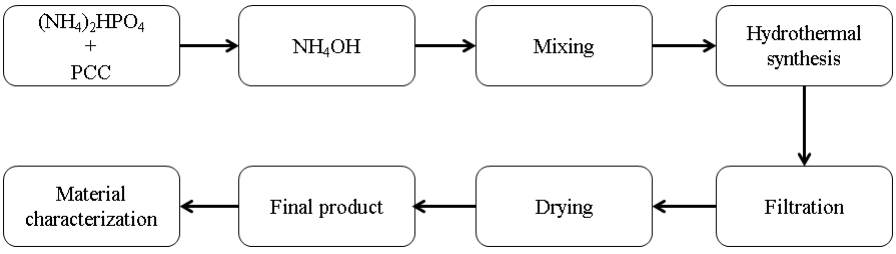

Figure-2. Set-up experiment of hydroxyapatite synthesis.

After the hydrothermal process was complete, the precursors produced were washed utilizing distilled water, which was then filtered utilizing Whatman paper no. 42. The residue produced after the filtration process is dried in an oven for 2 hours at 110°C to form the final product. Moreover, the final product's characterization was obtained using Fourier transforms infrared spectroscopy (FTIR), scanning electron microscopy (SEM), and X-ray diffraction (XRD) tests. XRD testing was carried out to analyze the phase contained in HAp using the Shimadzu XRD-7000. Note that the test results were analyzed using the Rietveld method with HighScore Plus software version 3.0e from PANalytical X'Pert, Cambridge, United Kingdom, to determine the crystal system, crystal size, and weight percentage (%). The diffraction line profiles description at Rietveld refinement was accomplished by employing the pseudo-Voigt function. Apart from that, the crystal sizes of the samples were calculated using The Williamson-Hall method [30]. The FTIR method was employed to distinguish the material's functional groups incorporated as well as to determine the molecular chain orientation in the HAp. In addition, the structural changes caused by the processing procedure, such as stretching or bending of the functional groups in the polymer, might be assessed using FTIR spectra.

Utilizing a Spectrum Two FTIR Spectrometer (USA), the functional groups in the HAp were detected, with the range of each spectrum being 400 to 4000 cm^{-1}. The Spectrum 10 ESTM™ software was employed to conduct the spectral correction of FTIR spectra. Additionally, the samples were observed morphologically utilizing an SEM (JSM-6510 Series Scanning Electron Microscope, Japan) at an accelerating voltage of 15 kV with a magnification of 15000x [31], [32].

RESULTS AND DISCUSSIONS

Figure-3 shows the X-ray diffraction (XRD) patterns for each hydroxyapatite (HAp) sample at various hydrothermal temperature conditions. According to Joint Committee of Powder Diffraction Standards (JCPDS) number 09-0432, all hydrothermal temperature variations demonstrated the dominance of HAp crystals. Other than that, calcium carbonate ($CaCO_3$) as an impurity was still found in all samples, which proved that not all $CaCO_3$ was converted to HAp, which was also found in previous research [33]–[37].

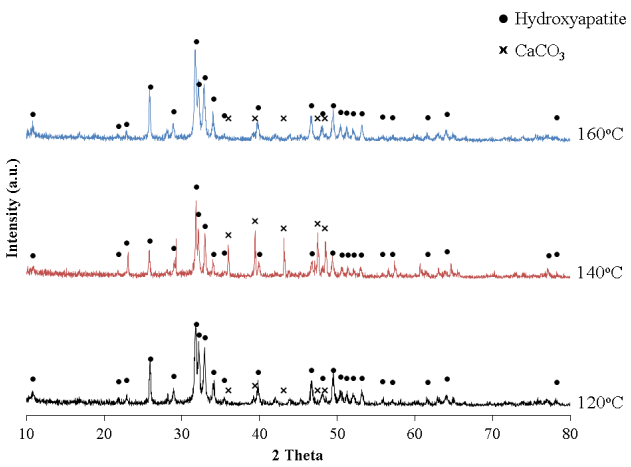

Figure-3. The samples' XRD patterns after being exposed to various hydrothermal temperatures.

Figures 4-6 show the Rietveld analysis findings employing the HighScore Plus software relying on XRD achieved from the test findings. Figure-4 depicts the XRD pattern on a powder synthesized by hydrothermal method for 14 hours at 120°C. Meanwhile, the XRD pattern illustrates that the hexagonal HAp phase was created with a 31.5 nm crystallite size as well as a 97.4% weight percentage. Nevertheless, the aragonite, calcite, and vaterite phases were still found at a weight percentage of 1.4%, 0.3%, and 0.8% at 120°C. In the hydrothermal process carried out at a temperature of 120°C, the total $CaCO_3$ (aragonite, calcite, and vaterite) as an impurity was 2.6%.

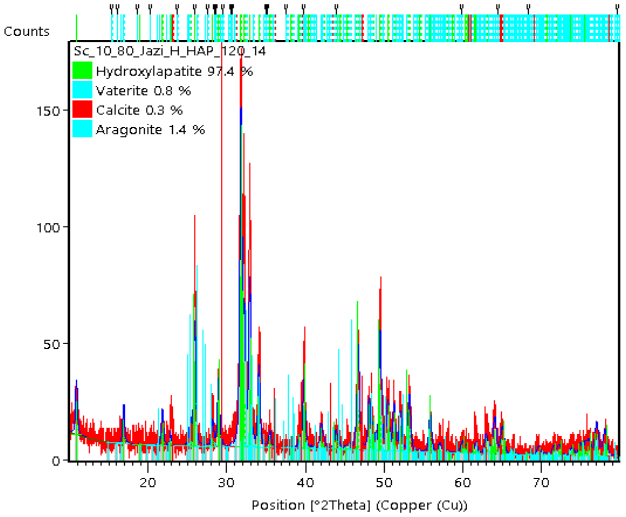

Figure-4. XRD pattern of samples exposed to hydrothermal temperatures of 120°C.

Figure-5 depicts the XRD pattern on a powder synthesized by hydrothermal method for 14 hours at 140°C. The XRD pattern illustrates that the hexagonal HAp phase was created with a 40.1 nm crystallite size as well as a 97.8% weight percentage. Nevertheless, the aragonite, calcite, and vaterite phases were still found at a weight percentage of 0.7%, 0.3%, and 1.2% at 140°C. In the hydrothermal process at a 140°C temperature, the total amount of $CaCO_3$ (aragonite, calcite, and vaterite) as an impurity was 2.2%. Note that this amount is lower than the impurity content produced in hydrothermal temperatures of 120°C.

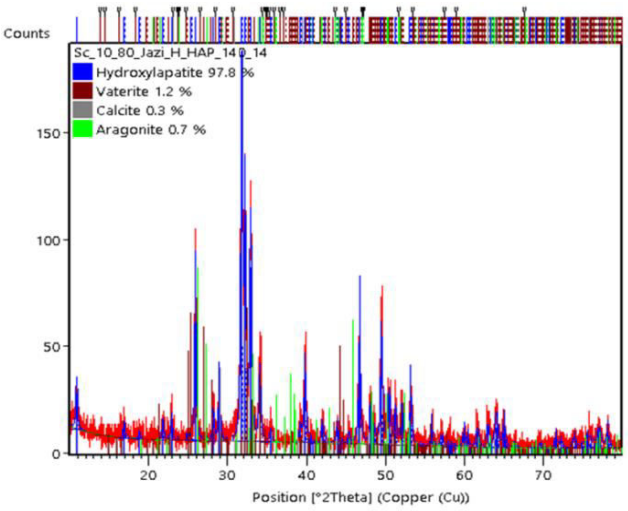

Figure-5. XRD pattern of samples exposed to hydrothermal temperatures of 140°C.

The XRD pattern on a powder that has been synthesized by hydrothermal method for 14 hours at 160°C is depicted in Figure-6. The hexagonal HAp phase was produced with a 46.4 nm crystallite size as well as a 99.3% weight percentage (%), as illustrated in the XRD

pattern. Nevertheless, the aragonite, calcite, and vaterite phases were still found at a weight percentage of 0.3%, 0.3%, and 0.1% at 160°C. In the hydrothermal process carried out at a 160°C temperature, the total amount of $CaCO_3$ (aragonite, calcite, and vaterite) as an impurity was 0.7%. This amount is the lowest compared to the impurity content produced in other hydrothermal temperature variations. The research findings prove that HAp is formed at all variations of hydrothermal temperature. However, a second phase is still being formed. In this study, the HAp phase diffraction peaks were observed at 2θ of 25.77°, 31.81°, 32.12°, 34.01°, 39.97°, 46.74°, and 49.38°. The study's findings are consistent with the literature [38].

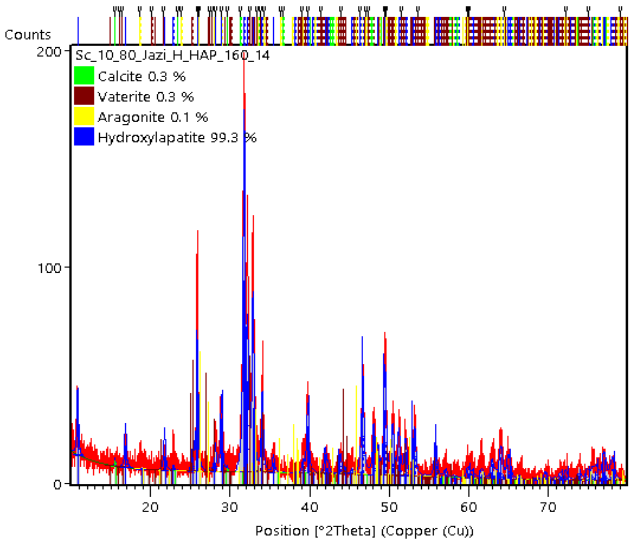

Figure-6. XRD pattern of samples exposed to hydrothermal temperatures of 160°C.

The hydrothermal temperature effect on the crystallite sizes, as well as weight percentage (%) with respect to the HAp formed, is shown in Figure-7. Sharper HAp peak intensities and increased crystallinity resulted from the hydrothermal temperature rise. Moreover, the hydrothermal temperature rise caused the diffraction peaks of the $CaCO_3$ (aragonite, vaterite, and calcite) to decrease. As the hydrothermal temperature functions, the peak intensity of the HAp diffraction peaks becomes greater or sharper. This proposed that the crystallinity (%) of the HAp also increased. The sizes of the crystallites also grew, as was documented in other research [38]–[40].

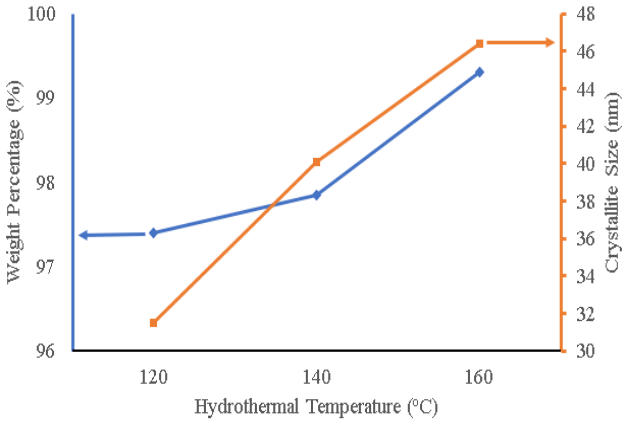

Figure-7. The hydrothermal temperature effect the crystallite size and weight percentage (%) of hydroxyapatite formed.

These research findings show that the greater the hydrothermal temperature used, the greater the weight percentage (%) of HAp is formed, having lower impurity content. The findings of this research depict that the greater the hydrothermal temperature utilized, the greater the weight percentage of HAp formed, and thus, the lower the impurity content [24], [30], [38]–[41]. The research findings demonstrated that the HAp crystallite size increased by increasing hydrothermal temperature. The hydrothermal process performed at temperatures of 120°C, 140°C, as well as 160°C formed HAp with crystallite sizes (nm) of 31.5, 40.1, and 46.4. Since the smaller apatite crystals have more activity when they bind with one another and develop down the C axis, the greater hydrothermal temperature promotes the creation of bigger crystals. The outcome of this investigation is consistent with those of the sources cited [39], [40]. The results of research conducted by Tkalčec *et al.* showed that large lattice strains were found in samples that were hydrothermal at lower temperatures. This is due to the incorporation of carbonate into the original apatite structure, which prevents crystallite growth. As the carbonate is removed with increasing hydrothermal temperature, the lattice strain becomes almost negligible, thereby promoting further crystal growth and causing an increase in crystallite size in the resulting hydroxyapatite [42]. Additionally, the HAp crystal system created in this research was unaffected by a rise in the hydrothermal temperature.

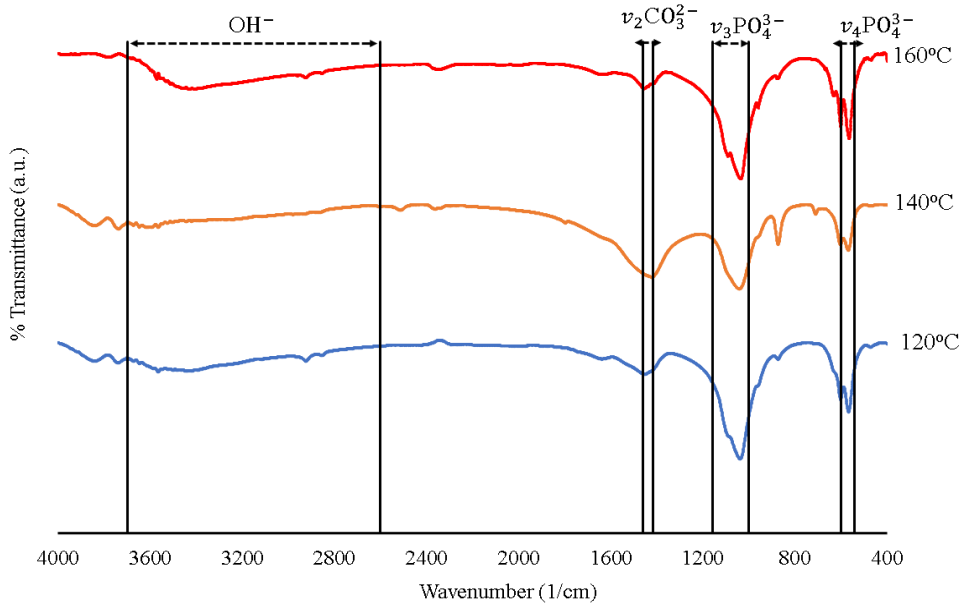

Figure-8. FTIR spectrums of the samples were exposed to different hydrothermal temperatures.

The Fourier transforms infrared spectroscopy (FTIR) test findings are illustrated in Figure 8. The peaks at 3570-2600 cm^{-1} showed the characteristic of hydroxyl (-OH) groups in nanoapatite crystals. Note that the appearance of peaks was in the range 1156-1000 cm^{-1} and 600-560 cm^{-1} because of the asymmetric stretching (υ2) and asymmetric bending (υ3) at PO_4^{3-} (phosphate group), which indicated the presence of free organic matter of HAp.

Meanwhile, the CO_3^{2-} presence is determined by the asymmetric bending vibration (υ2) presence in the range of 1460-1418 cm^{-1} [43], [44]. In the HAp produced by the hydrothermal method at a temperature of 120°C, the presence of -OH, PO_4^{3-}, and CO_3^{2-} were indicated by the presence of peaks at 3567.04, 1038.94, 567.78, and 1456.18 cm^{-1}. The presence of -OH, PO_4^{3-}, and CO_3^{2-} in HAp produced by the hydrothermal method at a temperature of 140°C was indicated by the presence of peaks at 3566.66, 1042, 569.39, and 1423.95 cm^{-1}. Meanwhile, for HAp produced by the hydrothermal method at a temperature of 160°C, the presence of -OH, PO_4^{3-}, and CO_3^{2-} was indicated by the presence of peaks at 3572.6, 1035.23, 565.12, and 1457.88 cm^{-1}.

The intensity of the peaks indicating the characteristics of the hydroxyl groups (-OH) in nanoapatite crystals decreased with increasing hydrothermal temperature. The research results obtained by Ryu et al. showed that the decrease in the peak of the hydroxyl group (-OH) in the apatite nanocrystals occurred due to the evaporation of water. The higher the hydrothermal temperature used, the more water evaporation will occur [45]. As the hydrothermal temperature rises, the intensity of the peaks showing the presence of hydroxyl groups in nanoapatite crystals decreases. The hydroxyl groups become more mobile and reactive as a result of the high temperature and pressure, leading to their dissociation and/or removal from the crystal lattice. This can lead to a drop in the total number of hydroxyl groups in the nanoapatite crystals, which is represented by a decrease in the intensity of the associated FTIR peaks. The decrease in intensity of the peaks reflecting the features of hydroxyl groups in nanoapatite crystals as the hydrothermal temperature increases are the result of the thermal decomposition of these groups under high temperature and pressure conditions [40], [46].

The higher the hydrothermal temperature employed, the sharper the peak at PO_4^{3-} and the peak at CO_3^{2-} disappeared. This is because when the hydrothermal temperature increases, the conditions become more aggressive and the nanoapatite crystal structure becomes more uniform. This leads to the formation of a sharper peak at PO_4^{3-} because the phosphate groups in the crystal lattice grow denser and more homogeneous. At the same time, the CO_3^{2-} peak disappeared as a result of the carbonate groups being removed from the crystal structure due to the high temperature. This indicates that the crystallinity of HAp is getting better, and the impurity content is getting smaller [42], [46]. In a study by Ebrahimi et al., the degree of crystallinity and intensity of the peak in the HAp increased as the temperature of the hydrothermal process increased [46].

Figure-9 (a-c) compares the HAp morphology synthesized by the hydrothermal method. At all variations in hydrothermal temperature, the resulting HAp has an irregular shape. In addition, the HAp particles mostly agglomerated due to the existence of water molecules that the drying process was unable to remove from the sample [47]. The findings of this study are consistent with those of prior findings [7], [23], [47]. Using seashells in HAp will produce irregular, nearly spherical, flat plates and rod-like morphology [7], [47].

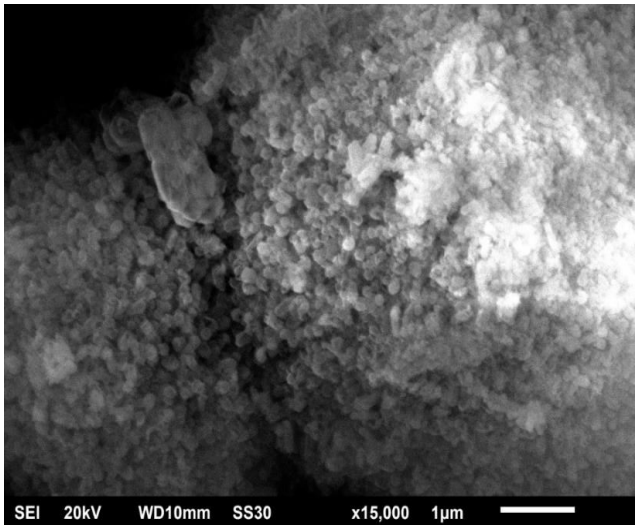

(a)

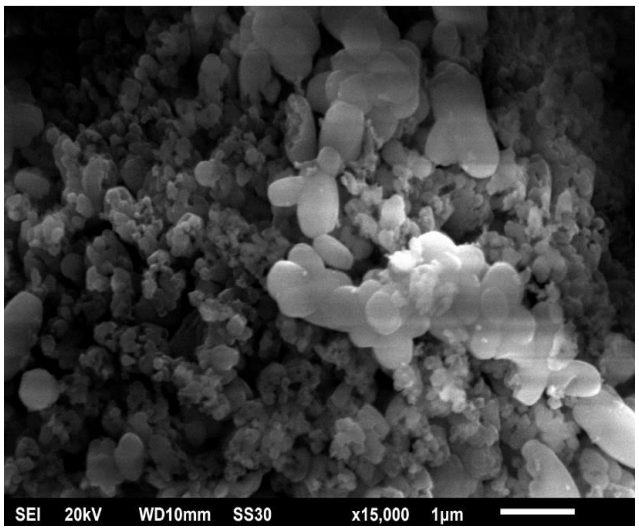

(b)

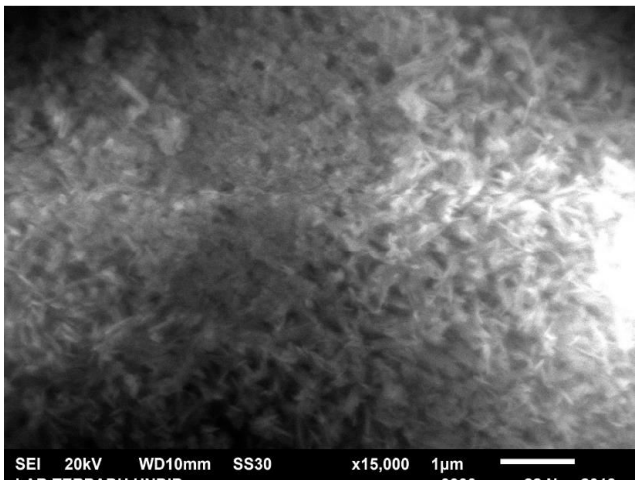

(c)

Figure-9. SEM images of samples exposed to various hydrothermal temperatures (a) 120℃, (b) 140℃, and (c) 160℃ under 15.000 magnifications.

CONCLUSIONS

The hydrothermal method has been employed with success at all temperature variations to synthesize hydroxyapatite (HAp) from green mussel shells utilizing precipitated calcium carbonate (PCC). In this study, the HAp produced in all variations has a hexagonal crystal system. The hydrothermal temperature affected the weight percentage (%), crystallite size, morphology, and the amount of impurities (%) in the resulting HAp. Other than that, the greater the hydrothermal temperature, the greater the weight percentage (%), while the larger the crystallite size in the HAp, the smaller the amount of impurities. The best results in this study were obtained at the hydrothermal temperature variation of 160℃. In this variation, the HAp produced has a crystallite size, weight percentage (%), and total impurities (%) of 46.4 nm, 99.3%, and 0.7%. Overall, the HAp produced in this study has an irregular morphology in all variations.

ACKNOWLEDGEMENTS

This research experiment was supported by the Faculty of Engineering, Semarang State University (UNNES), through a Penelitian Dasar Grant in 2023 with contract number 20.17.4/UN37/PPK.05/2023. In addition, the authors would like to thank Tarumanagara University for allocating funds under the International Research Collaboration Scheme.

CONFLICTS OF INTEREST: The authors declare that they have no conflict of interest.

REFERENCES

[1] S.-L. Bee and Z. A. A. Hamid. 2020. Hydroxyapatite derived from food industry bio-wastes: Syntheses, properties and its potential multifunctional applications. Ceram. Int. 46(11): Part A, 17149-17175.

[2] M. Sari and Y. Yusuf. 2018. Synthesis and characterization of hydroxyapatite based on green mussel shells (perna viridis) with the variation of stirring time using the precipitation method. IOP Conf. Ser. Mater. Sci. Eng. 432(1).

[3] K. Lin and J. Chang. 2015. Structure and properties of hydroxyapatite for biomedical applications. in Hydroxyapatite (HAp) for Biomedical Applications, Woodhead Publishing Series in Biomaterials. pp. 3-19.

[4] J. K. Odusote, Y. Danyuo, A. D. Baruwa, and A. A. Azeez. 2019. Synthesis and characterization of hydroxyapatite from bovine bone for production of dental implants: J. Appl. Biomater. Funct. Mater. 17(2).

[5] I. Saleh, S. Syamsir, V. Pramaningsih and H. Hansen. 2021. The use of green mussel as bioindicator of heavy metal pollution in Indonesia: a review. Environ. Anal. Heal. Toxicol. 36(4): e2021026-0.

[6] R. Ismail *et al*. 2021. The Effect of Hydrothermal Holding Time on the Characterization of Hydroxyapatite Synthesized from Green Mussel Shells. J. Adv. Res. Fluid Mech. Therm. Sci. 80(1): 84-93.

[7] N. A. S. Mohd Pu'ad, P. Koshy, H. Z. Abdullah, M. I. Idris and T. C. Lee. 2019. Syntheses of hydroxyapatite from natural sources. Heliyon. 5: 1-14.

[8] G. Borciani, T. Fischetti, G. Ciapetti, M. Montesissa, N. Baldini and G. Graziani. 2023. Marine biological waste as a source of hydroxyapatite for bone tissue engineering applications. Ceram. Int. 49(2): 1572-1584.

[9] G. T. El-Bassyouni, S. S. Eldera, S. H. Kenawy and E. M. A. Hamzawy. 2020. Hydroxyapatite nanoparticles derived from mussel shells for in vitro cytotoxicity test and cell viability. Heliyon. 6(6): e04085.

[10] L.-H. Huang, X.-Y. Sun and J.-M. Ouyang. 2019. Shape-dependent toxicity and mineralization of hydroxyapatite nanoparticles in A7R5 aortic smooth muscle cells. Sci. Rep. 9(1): 18979.

[11] R. Akhwady and R. Bayuaji. 2017. The Influence of Clamshell on Mechanical Properties of Non-Structure Concrete as Artificial Reef. Asian J. Appl. Sci. 05(02): 2321-0893.

[12] M. H. Azarian and W. Sutapun. 2022. Biogenic calcium carbonate derived from waste shells for advanced material applications: A review. Front. Mater. 9(November): 1-17.

[13] H.-C. Tsai, S.-L. Lo and J. Kuo. 2011. Using pretreated waste oyster and clam shells and microwave hydrothermal treatment to recover boron from concentrated wastewater. Bioresour. Technol. 102(17): 7802-7806.

[14] A. S. Saragih, A. Pamungkas and A. Noviyanto. 2020. Synthesis of hydroxyapatite from indonesian green mussels (Perna viridis) via precipitation methods. Key Eng. Mater. 833 KEM: 199-203.

[15] A. Hart. 2020. Mini-review of waste shell-derived materials applications. Waste Manag. Res. 38(5): 514-527.

[16] B. P. Kafle. 2020. Chapter 6 - Introduction to nanomaterials and application of UV–Visible spectroscopy for their characterization. In Chemical Analysis and Material Characterization by Spectrophotometry, B. P. B. T.-C. A. and M. C. by S. Kafle, Ed. Elsevier. pp. 147-198.

[17] S. P. Ghawade, K. N. Pande, S. J. Dhoble, and A. D. Deshmukh. 2022. 11 - Tuning the properties of ZnS semiconductor by the addition of grapheme. in Woodhead Publishing Series in Electronic and Optical Materials, V. B. Pawade, S. J. Dhoble, and H. C. B. T.-N. C. S. and their O. A. Swart, Eds. Woodhead Publishing. pp. 351-381.

[18] T. Laonapakul. 2015. Synthesis of hydroxyapatite from biogenic wastes. Kku Eng. J. 42(3): 269-275.

[19] S. C. Cox. 2015. Synthesis Method of Hydroxyapatite Author : Sophie Cox. Ceram, no. January 2014, pp. 1-7.

[20] S. C. Cox, R. I. Walton and K. K. Mallick. 2015. Comparison of techniques for the synthesis of hydroxyapatite. Bioinspired, Biomim. Nanobiomaterials. 4(1): 37-47.

[21] D. F. Fitriyana, R. Ismail, Y. I. Santosa, S. Nugroho, A. J. Hakim and M. Syahreza Al Mulqi. 2019. Hydroxyapatite Synthesis from Clam Shell Using Hydrothermal Method : A Review. 2019 Int. Biomed. Instrum. Technol. Conf. IBITeC 2019, pp. 7-11, Oct.

[22] H. Onoda and S. Yamazaki. 2016. Homogenous hydrothermal synthesis of calcium phosphate with calcium carbonate and corbicula shells. J. Asian Ceram. Soc. 4(4): 403-406.

[23] Y. Azis, N. Jamarun, Zultiniar, S. Arief and H. Nur. 2015. Synthesis of hydroxyapatite by hydrothermal method from cockle shell (Anadara granosa). J. Chem. Pharm. Res. 7(5): 798-804.

[24] Y. Zhu, L. Xu, C. Liu, C. Zhang and N. Wu. 2018. Nucleation and growth of hydroxyapatite nanocrystals by hydrothermal method. AIP Adv. 8(8): 085221.

[25] BPS. 2021. Badan Pusat Statistik.

[26] R. Febrida *et al*. 2021. Synthesis and Characterization of Porous CaCO 3 Vaterite Particles by Simple Solution Method. Materials (Basel). 14(16): 4425, 1-17.

[27] K. Tanaka, A. Tsuchiya, Y. Ogino, Y. Ayukawa, and K. Ishikawa. 2022. Comparison of calcite and vaterite as precursors for CO3Ap artificial bone fabrication through a dissolution-precipitation reaction. Ceram. Int. 48(18): 26425-26431.

[28] R. Ismail *et al*. 2021. The potential use of green mussel (Perna Viridis) shells for synthetic calcium carbonate polymorphs in biomaterials. J. Cryst. Growth. p. 126282.

[29] R. Ismail *et al*. 2022. Synthesis and Characterization of Calcium Carbonate Obtained from Green Mussel and Crab Shells as a Biomaterials Candidate. Materials (Basel). 15(16): 1-15.

[30] R. Rusiyanto *et al*. 2021. Effect of Sintering Temperature on the Physical Properties of Ba0.6Sr0.4TiO3 Prepared by Solid-State Reaction. Int. J. Automot. Mech. Eng. 18(2): 8752-8759-8752-8759.

[31] D. F. Fitriyana *et al*. 2020. The Effect of Compressed Air Pressure and Stand-off Distance on the Twin Wire Arc Spray (TWAS) Coating for Pump Impeller from AISI 304 Stainless Steel. Springer Proc. Phys. 242(June): 119-130.

[32] D. F. Fitriyana *et al*. 2022. The Effect of Post-Heat Treatment on the Mechanical Properties of FeCrBMnSi Coatings Prepared by Twin Wire Arc Spraying (TWAS) Method on Pump Impeller from 304 Stainless Steel. J. Adv. Res. Fluid Mech. Therm. Sci. 2(2): 138-147.

[33] M. Sirait, K. Sinulingga, N. Siregar and Y. F. Damanik. 2020. Synthesis and characterization of hydroxyapatite from broiler eggshell. AIP Conf. Proc. 2221: 1063-1066.

[34] M. Sawada, K. Sridhar, Y. Kanda and S. Yamanaka. 2021. Pure hydroxyapatite synthesis originating from amorphous calcium carbonate. Sci. Rep. 11(1): 1-9.

[35] M. Kamitakahara, T. Nagamori, T. Yokoi and K. Ioku. 2015. Carbonate-containing hydroxyapatite synthesized by the hydrothermal treatment of different calcium carbonates in a phosphate-containing solution. J. Asian Ceram. Soc. 3(3): 287-291.

[36] D. Pham Minh *et al*. 2018. Hydroxyapatite starting from calcium carbonate and orthophosphoric acid: Synthesis, characterization, and applications. J. Mater. Sci. 49(12): 4261-4269.

[37] F. Cestari, F. Agostinacchio, A. Galotta, G. Chemello, A. Motta and V. M. Sglavo. 2021. Nano-hydroxyapatite derived from biogenic and bioinspired calcium carbonates: Synthesis and in vitro bioactivity. Nanomaterials. 11(2): 1-14.

[38] J. Chen, Z. Wen, S. Zhong, Z. Wang, J. Wu and Q. Zhang 2015. Synthesis of hydroxyapatite nanorods from abalone shells via hydrothermal solid-state conversion. Mater. Des. 87: 445-449.

[39] H. Nosrati, R. Sarraf-Mamoory, D. Q. S. Le and C. E. Bünger. 2020. Enhanced fracture toughness of three dimensional grapheme - hydroxyapatite nanocomposites by employing the Taguchi method. Compos. Part B Eng. Vol. 190.

[40] S. Ebrahimi, C. S. S. M. Nasri and S. E. Bin Arshad. 2021. Hydrothermal synthesis of hydroxyapatite powders using Response Surface Methodology (RSM). PLoS One. 16(5).

[41] D. F. Fitriyana, H. Suhaimi, Sulardjaka, R. Noferi and W. Caesarendra. 2020. Synthesis of Na-P Zeolite from Geothermal Sludge. Springer Proc. Phys. 242: 51-59.

[42] E. Tkalčec, J. Popović, S. Orlić, S. Milardović and H. Ivanković. 2014. Hydrothermal synthesis and thermal evolution of carbonate- fluorhydroxyapatite scaffold from cuttlefish bones. Mater. Sci. Eng. C. 42: 578-586.

[43] K. C. Vinoth Kumar *et al*. 2021. Spectral characterization of hydroxyapatite extracted from Black Sumatra and Fighting cock bone samples: A comparative analysis. Saudi J. Biol. Sci. 28(1): 840-846.

[44] J. Triyono, R. Adityawan, P. Dananjaya, D. F. Smaradhana and A. Masykur. 2021. Characterization and biodegradation rate of hydroxyapatite/shellac/sorghum for bone scaffold materials. Cogent Eng. 8(1).

[45] G. U. Ryu, G. M. Kim, H. R. Khalid and H. K. Lee. 2019. The Effects of Temperature on the Hydrothermal Synthesis of Hydroxyapatite-Zeolite Using Blast Furnace Slag. Materials (Basel). 12(13).

[46] S. Ebrahimi and C. S. Sipaut. 2022. Synthesis of Hydroxyapatite/Bioglass Composite Nanopowder Using Design of Experiments. Nanomaterials. 12(13).

[47] M. Z. A. Khiri *et al*. 2016. The usability of ark clam shell (Anadara granosa) as calcium precursor to produce hydroxyapatite nanoparticle via wet chemical precipitate method in various sintering temperature. Springer Plus 2016 51. 5(1): 1-15.